Minimization of fine particles emission from biomass combustion

Liquefaction, combustion additives and cyclone separators

Sriram Hariharakrishnan
sriramh.2009@gmail.com
Instituto Superior Técnico, Universidade de Lisboa, Lisbon, Portugal

October 2017

ABSTRACT

The global energy demand is ever-increasing due to factors such as population increase, and fossil fuels have played a major role in meeting these needs. However, the adverse environmental effects of fossil fuels call for increased use of renewable energy sources such as biomass. Biomass combustion is a common alternative of producing energy but the high concentration of fine particles in the flue gas can be a problem. Acid-catalysed liquefaction of lignocellulosic biomasses such as pinewood, olive stone/pits, olive bagasse, grape seeds, and rice husk was studied as a pre-treatment to combustion to remove the inorganic ash-forming species, while producing a liquid biofuel more easily burned. Liquefaction at 160ºC using 2-Ethylhexanol as solvent was optimised to have a high biomass/solvent ratio (1:1). The highest conversion achieved using this ratio under optimised conditions was ≈55% while 60 to 70% of the initial inorganic content of the biomass was removed in the liquefaction, thus proving its potential as a pre-treatment to decrease particles emissions.

Alternatively, to decrease the fine particles emitted as fly ash during combustion, some additives were selected and tested for their ability to capture fine particles and/or to increase the particle size of the ash particles. From the preliminary tests, TiO_2 showed promising results in decreasing particulate emissions, particularly PM_1.

Aspen Plus was used to simulate multicyclones, helical and spiral cyclones. These cyclones design were evaluated and further optimised for better performance. It was possible to obtain 16% efficiency increase.

Keywords: Biomass liquefaction; particulate emissions; combustion; additives; cyclones.

1. INTRODUCTION

1.1. Biomass combustion

Biomass combustion technologies have been around for several decades but there are many obstacles such as high moisture content, low bulk density, ash formation, etc. The high moisture content of biomass causes poor ignition and lowering of temperature during combustion. In addition to this, high moisture content also causes high transportation and storage costs. Biomass has low bulk density causing logistical problems and storage hazards such as spontaneous combustion due to high surface area and volume. Biomass also has a lower energy density compared to coal. These problems can be solved by pre-treatment and densification of biomass. Grinding is one of the pre-treatment techniques used to decrease the energy consumption during densification process and to give denser products as output during compaction [Clarke and Preto, 2011]. Drying of the biomass is needed to decrease the moisture content which in turn increases the density and durability of the biomass feedstock [Clarke and Preto, 2011]. The biomass needs certain moisture content for ease of compaction and above that level of moisture, the durability and density of the biomass is reduced. Also, the density and durability depends on the natural binding agents of the biomass material. Sometimes, binding agent additives such as vegetable oil, starch, clay, wax, etc. are added for effective compaction of biomass to pellets, bales, etc [Clarke and Preto, 2011]. Steaming is a method of pre-treatment where addition of steam aids in the release and activation of the natural binders in the biomass [Clarke and Preto, 2011]. Another pre-treatment process is torrefaction. Torrefaction is a form of mild pyrolysis at temperature of about 200 to 320 ˚C which is carried out under atmospheric pressure but in the absence of oxygen [Chew, 2011]. During this process, the water contained in the biomass and the superfluous volatiles are released and the polymeric part containing cellulose, hemicellulose, lignin partly decomposes [Chew, 2011]. The final product from this process is a denser biomass commonly called bio-char in literature. This process consumes more energy which is a demerit in the overall Life cycle impact of the energy from agricultural and forest residues [Clarke and Preto, 2011]. This can however be offset by using the volatiles from this process to provide heat for torrefaction and by minimizing the loss of low value heat by optimizing the process further. The pre-treatment processes provide value addition to the biomass by giving it higher energy density, more homogeneous composition, hydrophobic behaviour, and less biological activity thus preventing the rotting of biomass [Chew, 2011]. Pyrolysis is also used as a pre-treatment to produce bio-oil and bio-char which can further be burned combusted [FAO]. However, a major demerit associated with this process is the high energy consumption [FAO]. The slurry of this bio-oil and bio-char may be used as combustion feedstock. As mentioned in the next item, another major problem with biomass is the typically high inorganic content which leads to problems such as slagging, fouling and agglomeration. Some biomass such as rice husk have higher silica content causing ceramic material like deposits which are hard to clean during blow down. Most biomasses have high potassium and Chlorine content. K content leads to lower ash melting temperatures and Cl content favours the formation of fly ash which is a major environmental concern regarding biomass combustion [Obernberger]. In this perspective, liquefaction is a potential pre-treatment to decrease the problems associated with the inorganic content before combustion, high moisture content of biomasses and to facilitate easier combustion by using bio-liquids instead of direct biomass combustion. In the literature, liquefaction has been studied widely as a pathway to liquid fuels and some chemicals but not as a pre-treatment before combustion.

1.2. Liquefaction

1.2.1. Liquefaction process

Liquefaction of biomass is a solvolytic process that is either acid-catalysed or base-catalysed, most commonly the former. During liquefaction, biomass gets degraded into smaller molecules by dissolution and reaction with a solvent, at atmospheric pressure and at temperature of 150 to 250 °C. Usually, one or more polyhydric alcohols are used as solvent [Li, 2015]. The structural and chemical composition of the biomass determines the mechanism and results of liquefaction. Any lignocellulosic biomass is composed mainly of three types of polymers- cellulose, hemicellulose and lignin and the composition of these in a lignocellulosic biomass influences the liquefaction process. Besides these polymers, comparatively small amounts of pectin, proteins, extractives and inorganic content constitute lignocellulosic biomass [Bajpai et al., 2016]. The liquefaction of amorphous cellulose, lignin and hemicellulose occurs fast in the initial stages of liquefaction process

due to their amorphous structure while crystalline cellulose undergoes liquefaction at a slower rate and continues till the end of the process due to its less accessibility to the solvent. As crystalline cellulose majorly constitutes the cellulose in lignocellulosic biomass, the conversion of cellulose is the limiting reaction in the liquefaction process [Li et al., 2015]. For example, the nucleophilic substitution is the reaction mechanism of one of the major reactions during acid-catalysed cellulose liquefaction in polyhydric alcohols as solvents forming levulinate [Li et al., 2015]. A large number of simultaneous competing reactions occur during liquefaction of lignocellulosic biomass. Recondensation reactions compete against the liquefaction reactions and decrease the process efficiency by forming more insoluble residues [Li et al., 2015]. Kobayashi et al. (2004) postulated that these recondensation reactions are due to reactions between depolymerized cellulose and degraded aromatic lignin derivatives. The most common way to decrease the menace of recondensation is to optimise the process parameters such as biomass to liquid ratio, solvent used, catalyst used, catalyst quantity, reaction time and temperature [Li et al., 2015]. The liquefaction products vary widely with the type of biomass used and the process parameters. As concluded by Zhang et al. (2007), the liquefied product from acid-catalysed bagasse liquefaction using ethylene glycol was composed of high molecular weight lignin degradation products, phenols, saccharides, alcohols, aldehydes, some acids and their esters while the liquefaction residue contained some lignin derivatives, undissolved cellulose and undissolved lignin.

12.2. Contemporary developments in biomass liquefaction

The conversion of biomass to liquids started out with hydrothermal liquefaction processes which are carried out at high temperature and high pressure. To name a few, Pittsburgh Energy Research Centre (PERC) process, Bureau of Mines (BOM) process and Lawrence Berkeley Laboratory (LBL) process belong to this category of hydrothermal liquefaction [Elliott]. In BOM process, comminuted biomass was slurried using tar oil with 20 to 30% biomass in the slurry [Tarelho et al., 2011]. This slurry was then reacted with carbon monoxide and aqueous sodium carbonate in a reactor for 20 to 90 minutes at 300 to 370 °C and at high pressure of 2000 to 4000 psig [Elliott]. LBL process is carried out under similar conditions as BOM process but the biomass is converted to aqueous slurry by acid hydrolysis without the need for predrying and comminution [Elliott]. Some processes use supercritical water or supercritical CO_2 as solvents to liquefy biomass. These hydrothermal liquefaction processes produce complex mixtures of biocrudes and it is an insurmountable task to upgrade and/or refine these crudes to pure chemicals [Zhang et al., 2007]. Also, the operational complexity and expense of these processes are quite high [Zhang et al., 2007]. Hence, mild liquefaction of biomass at low to moderate temperatures and atmospheric pressure is more interesting to convert biomass to liquid with significantly reduced operational complexity and costs [Zhang et al., 2007]. Ting Zhang et al. (2007) studied the sulphuric acid catalysed liquefaction of bagasse in ethylene glycol at 190 °C and atmospheric pressure and found that the process they used has a high potential to produce biofuels and some chemicals from biomass. Many similar liquefaction processes at similar range of temperatures and atmospheric pressure are found in scientific literature. The commonly used solvents are glycerol, ethylene glycol, diethylene glycol, 2-Ethyl hexanol and polyethylene glycol among other polyhydric alcohols [(Hu et al., 2013), (Mateus et al., 2015)]. Most of these processes are carried out at low biomass to solvent ratios of 1:3 to 1:5 [Li et al., 2015]. The solvent used and the lignocellulosic composition of the biomass highly influence the liquefaction efficiency. For instance, sulphuric acid catalysed liquefaction gave liquefaction rates in decreasing order from bagasse, cotton stalks to wheat straw [Li et al., 2015]. Biomass with high lignin and hemicellulose content show greater liquefaction rates due to the ease of accessibility of their amorphous structure by solvents. Using a mixture of 4:1 w/w PEG400 (MW. 400 g/mol) to glycerol as solvent showed high liquefaction efficiencies and decreased occurrence of recondensation reactions [Li et al., 2015]. Besides polyhydric alcohols, Ethylene carbonate and Propylene carbonate are also used as solvents with good efficiency in some cases [Yamada and Ono, 1999]. Shengjun Hu et al. (2012) studied the use of crude glycerol from biodiesel production as a solvent and concluded that it is a potential alternative for expensive petroleum derived liquefaction solvents that are currently used. The most common catalyst used in liquefaction processes is concentrated sulphuric acid and the catalyst loading of 1 to 3% sulphuric acid exhibits optimum liquefaction behaviour in most cases. Though there are base catalysed liquefaction reactions, these usually require higher temperatures than acid-catalysed liquefaction [Li et al., 2015]. There are studies about using several other catalysts. For instance, Tang et al. (2017) used 15 wt. % of Zn supported on ZSM-5 as catalyst to liquefy oil palm empty fruit bunch. Besides these stand-alone liquefaction processes, there are investigations on ultrasonic, microwave and/or plasma aided liquefaction processes. The studies by Lu et al. (2016) concluded that microwave-ultrasonic assisted liquefaction of woody biomass intensified the heat & mass transfer, significantly reduced the liquefaction time and halved the solvent dosage. Xi et al. (2017) studied the application of plasma electrolysis in sulphuric acid catalysed liquefaction of sawdust using a mixture of PEG200 and glycerol as solvent. It was found that the liquefaction yield reached 99.08% in 5 minutes under optimal biomass to solvent ratio of 1:7.12 implicating the good potential of plasma electrolysis in fast biomass liquefaction. Pinewood sawdust is the most studied lignocellulosic biomass in terms of liquefaction though liquefaction of several other biomasses such as cork, potato peels, eucalyptus bark and coffee grounds have been studied and documented [(Mateus et al., 2016), (Mateus et al., 2017)]. Liquefaction of olive stone was studied by Cuevas et al. (2008) through autohydrolysis - enzymatic hydrolysis pathway and showed good potential for producing bioethanol through this process. However, there is hardly any research on direct solvolytic liquefaction of olive stones. Also, most documented research focus on optimising biomass liquefaction to produce polyurethane foams or to upgrade to bio-oils. Hardly any focus has been placed on investigating liquefaction in the context of a pre-treatment method before combustion in lieu of direct combustion of biomass.

1.3. Additives to reduce fine particle emissions

Combustion additives are commonly classified based on their chemical composition – specifically, their reactive component, into Calcium additives, Phosphorous additives, Aluminium additives, Aluminium-Silicate additives and Sulphur additives, with the first four possibly applicable for reduction of particle emissions [Bäfver et al., 2011]. Bauxite ore containing aluminium oxide or hydroxide is a prime example of Al-based combustion additives; Calcium carbonate and calcium hydroxide are examples of Ca-based combustion additives; Phosphoric acid, Calcium dihydrogen phosphate and phosphorous rich sewage sludge are examples of P-based combustion additives; Kaolin and bentonite are examples of Aluminium-silicates based additives. Bäfver et al. (2011) opine that Al-Si additives and P-based additives can decrease the PM emissions; Al-based additives are less effective than Al-Si based additives and Ca-based additives may decrease PM emissions from P-rich fuels such as oat grain, while they apparently have no effect on PM emissions from Si-rich fuels such as straw and woody biomass. The effects of additives, obviously, depend on their reactions with the problematic ash forming components during combustion. K is the main cause of PM in fly

ash during combustion of most biomasses. PM emissions are controlled by additives either by chemical adsorption and interaction or by physical adsorption, with former being more common. Despite the complex nature of the reactions between additives and ash components and the seemingly impossible task of controlling their behaviour, there are several studies on the reaction mechanisms of additives with ash from different types of coals, biomasses and oils. Wang et al. (2012) summarize the main reactions between additives and K containing compounds formed during combustion, some of which are shown as follows.

$Al_2O_3.xSiO_2 + 2KCl + H_2O \rightarrow K_2O.\ Al_2O_3.xSiO_2 + 2\ HCl_{(g)}$...(1)

$2KCl + H_2O_{(g)} + Al_2O_3 \longrightarrow 2KAlO_2 + \ HCl_{(g)}$ ...(2)

$2\ KCl + SiO_2 + H_2O \longrightarrow \ K_2O.SiO_2 + 2\ HCl_{(g)}$ ... (3)

$SO_3 + 2KCl + H_2O_{(g)} \longrightarrow 2HCl_{(g)} + K_2SO_4$ … (4)

$KCl_{(g)} + CaHPO_4.2H_2O \rightarrow CaKPO_4 + 2\ H_2O + HCl_{(g)}$ ... (5)

In summary, PM emissions can be controlled by preventing the reaction of KCl with other ash components and/or capture the fine ash particles before their elutriation. The compounds resulting from the reactions between additive and ash should have a high melting point so as not to create problems during blow down operation. This aspect is analysed by studying the phase diagrams of these compounds. Additives can be added either together with fuels or midway during combustion. When Davidsson et al. (2007) studied the combustion of forestry residues in a CFB boiler, they added kaolin to the particle seal of the boiler and found out that most of the kaolin was elutriated along with flue gas to the ESP indicating that pre-blending of kaolin with biomass could be tried to solve this elutriation problem. There are significantly more studies about additives to reduce slagging and corrosion from coal as well as biomass combustion than about additives to decrease PM emissions. However, there are some studies that address additives for PM emissions worth noting and the results of some of those are described in brief as follows. Höfer et al. (2016) concluded from their studies on additives during wood and straw combustion that the additives Al_2O_3, a blend of 46% Al_2O_3, 44% $CaCO_3$, 10% $CaHPO_4$, and another blend of 46% Al_2O_3, 44% $MgCO_3$, 10% $MgHPO_4$ help to bind problematic species and reduce PM emissions. Fournel et al. (2015) studied combustion of reed canary grass blended with 50 wt. % wood and 3 wt. % fuel additives such as aluminium silicates (sewage sludge), calcium (limestone) and sulfur (lignosulfonate) based additives and found that combustion of these blends resulted in 17%–29% decrease of PM concentrations compared to pure reed canary grass. A report by Boman et al. (2012) indicates that kaolin has a good effect in decreasing PM emissions from combustion of many different types of biomass. Ninomiya et al. (2009) concluded that the use of Ca or Mg-based additives to coal combustion could result in the decrease of $PM_{2.5}$ and PM_1 emissions by improving the coalescence of fine particles. The effects of similar additives on PM from biomass combustion could be studied. There are more combustion additives than the common Al, Al-Si, Ca and P-based additives. For instance, Wiinikka et al. (2009) concluded from their study on straw combustion that the addition of an optimum amount of TiO_2 as additive reduced the vaporization of K by approximately 40 to 50% indicating its great potential in reduction of PM emissions. Besides their effect on combustion, additives are chosen having in mind the criteria such as absence of increased environmental toxicity due to adding it to combustion, stability of resultant compounds at high temperature and overhead cost of using the additives.

1.4. Downstream emissions reduction

There are different equipment for post combustion particle capture. Torbel specializes in manufacturing cyclones and surface filters. Due to the pertinence to this work, the design of cyclones will be explained in detail. Cyclone separators use the principle of forcing the gas towards a wall and use centrifugal force and gravitational force to collect particles. Cyclones can be categorized as high efficiency, conventional and high throughput cyclones based on their dimensions. There are several configurations of cyclones based on their dimensions. In the field of cyclone design, all cyclone dimensions are commonly normalized as a factor of the barrel diameter (D) of the cyclone as shown in Figure 1. The widely known configurations are Stairmand, Swift-High, Swift-General, Shepherd & Lapple and Peterson & Whitby cyclones [UF]. The normalized dimensions of these cyclones are as shown in Table 1. Here, in Figure 1, K_a, K_b, K_s, K_B, K_H, K_h, K_{D_e} are normalising factors for the respective parameters which are described in Table 1.

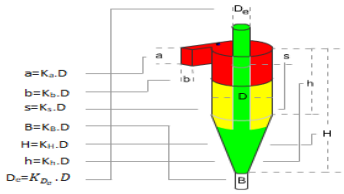

Figure 1: Normalized dimensions of a typical cyclone separator [UF]

Pressure drop in a cyclone is an important parameter that is considered during the design. Pressure drop can be calculated fairly accurately using Stairmand's equation, as shown below, but it represents the pressure drop due to clean gas without particle loading and hence correction factor has to be applied for depending on the cyclone design [NPTEL].

$$\Delta P = \frac{\rho_g}{203}\{V_i^2\left[1 + 2\emptyset^2\left(\frac{2r_t}{r_e} - 1\right)\right] + 2V_o^2\} \quad \rightarrow (6)$$

In the above equation, ρ_g is the gas density, V_i is the velocity of the gas at cyclone inlet, V_o is the velocity of the gas at cyclone gas outlet, r_t is the radius of circle to which the centre line of the inlet is tangential, r_e is the radius of the cyclone gas outlet, and ϕ is cyclone pressure drop factor which is given by Equation (7) shown below [NPTEL].

$$\phi = f_c(^{A_s}/_{A_i}) \rightarrow (7)$$

In the above equation, A_i is the area of cyclone inlet, and A_s is the surface area of cyclone that is exposed to the spinning gas inside the cyclone. Since, it is highly complex to theoretically compute A_s, it is taken to be equal to the surface area of an equivalent cylinder with same diameter as the cyclone body diameter and same height as the overall height of the cyclone [NPTEL]. As explained before, the collection efficiency of a cyclone is influenced by several parameters such as particle size, density, velocity of the gas, pressure drop in the cyclone, cyclone dimensions, surface characteristics of the material of the cyclone, particle loading in the gas, number of revolutions of the gas inside the cyclone, gas viscosity, leakage of air into the cyclone along with the gas, etc. In summary, the collection efficiency can be defined as a function of incoming gas properties, particle characteristics and cyclone design.

Table 1: Normalized dimensions of common cyclone configurations [UF]

Symbol	Description	High efficiency		Conventional	High throughput	
		Stairmand	Swift-High	Shepherd & Lapple	Swift-General	Peterson & Whitby
a	Inlet height	0.5D	0.44D	0.5D	0.5D	0.583D
b	Inlet width	0.2D	0.21D	0.25D	0.25D	0.208D
s	Outlet length	0.5D	0.5D	0.625D	0.6D	0.583D
B	Dust outlet diameter	0.2D	0.21D	0.25D	0.25D	0.208D
H	Overall height	4D	3.9D	4D	3.75D	3.17D
h	Cylinder height	1.5D	1.4D	2D	1.75D	1.33D
D_e	Gas outlet diameter	0.5D	0.4D	0.5D	0.5D	0.5D

There is no unified method of performing the design calculations for a cyclone separator and it is possible to use several approaches to explain the cyclone design calculations. Every method has its own merits and demerits depending on the process parameters and

the cyclone design for which it is applied to. Some of these methods are modelled based on experimental results and some of these are derived theoretically based completely on empirical concepts. The most practical method is Muschelknautz method [Elsayed, 2011]. Besides theoretical methods, calculations can be performed on a case by case basis using numerical modelling and/or CFD software for more accurate results [Elsayed, 2011]. The simulation and/or design of cyclones to suit the needs of a specific process plant can be easily performed using a process simulation software package such as Aspen Plus, Chemcad, etc. The results from the simulation runs in Aspen can be exported to Microsoft Excel for further interpretation and presentation of results. In this thesis, Aspen Plus V8.4 is used for this purpose. Aspen Plus is a software package created by Aspen Tech to design, simulate and optimize process models to efficiently design and operate process plants. Simulation and design of cyclones and other end of pipe PM capture equipment can be done using the solids handling block of Aspen Plus. Aspen Plus provides two modes of solid handling which are design and simulation. Aspen Plus is versatile to a large extent and has a lot of simulation features. The pertinent steps involved are explained in brief as follows. In simulation mode, the performance of a cyclone with known dimensions at predefined parameters can be evaluated whereas in design mode, Aspen Plus gives the design parameters of cyclone/multicyclone depending on the input conditions and required performance. The main steps in using Aspen solids handling by cyclones are setup, flowsheet, streams, blocks, and results. Setup is where the user can input the data regarding the unit system to be used, materials to be used in process streams, their properties, etc. Flowsheet is the core part where the process flow diagram is drawn. In the streams, the user has to define the materials, properties and process conditions of all the input and output streams. In blocks, the process parameters pertinent to all the process equipment involved and the calculation method to be used are established. Then the simulation is run to get the results. Aspen Plus contains several calculation methods for cyclone separators, namely, Muschelknautz, Leith-Licht, Shepherd & Lapple, modified Leith-Licht, Dietz, Mothes & Loffler and user-specified method. Some of these methods are explained in brief as follows.

Leith-Licht model works under the assumptions that the gas flow is intermediate to free and forced vortex flow, the trajectories of gas inside the cyclone are circles, particle-gas slip velocity is only radial, Stoke's law, plug-flow and mixed-flow models govern the radial force on a particle and the particles have negligible radial acceleration [Clift et al., 1991]. Muschelknautz model is based on the main assumption that the pressure loss inside the cyclone is caused by wall friction and irreversible losses in the vortex with the latter dominating the former in most cases [Elsayed, 2011]. According to Dietz model, a cyclone comprises three regions – entrance, downflow and core [Dirgo and Leith, 1985]. The entrance region is the space around the gas outlet at the top; downflow is the region of vortex; and the core is the region formed from extension of the gas outlet to the bottom of cyclone. In this work, Muschelknautz, Shepherd & Lapple, and Mothes-Loffler methods were used in Aspen Plus.

2. MATERIALS AND METHODS

2.1. Liquefaction

The biomass needed for liquefaction experiments – pinewood, olive stone, olive bagasse, and grape seeds were provided by Torbel whereas rice husk was procured from another source by Dr. Margarida Mateus. The pinewood here was the waste from forestry products; olive stones are the broken pits of olive fruits left after a second extraction of oil; olive bagasse is the same as olive stone but it contained fine powders from broken olive stones in addition to the olive stones itself; and grape seeds were the seeds left over from grapes after extraction and separation of the pulp in wineries. Except pinewood, all these other biomasses were used with the same size as received, in liquefaction experiments. Pinewood chips from Torbel were too big to be used in liquefaction and so, it was grinded to a particle size below 6 mm. In most of the liquefaction experiments, the solvent used was either 2-Ethyl hexanol (2EH) or a 1:1 w./w. mixture of 2EH and Diethylene Glycol (DEG) [this mixture is hereafter referred to as 'DEEH']. The catalyst used in all liquefaction experiments was p-Toluene Sulfonic acid (pTSA). In some experiments, Hydroquinone (HQ) was used as a stabilizer to test its effectiveness in preventing the occurrence of repolymerisation reactions. The sources of these reagents are as follows: Acetone – LabChem, 99.6% purity; DEG – Resiquimica, p.a. grade (>99%); pTSOH – Resiquimica, reagent grade (98%); and 2EH – Sigma-Aldrich, food grade (>99%). All the liquefaction experiments were carried out at 160 °C and ambient pressure. The procedure for this purpose was based on previous pinewood liquefaction studies at IST. The catalyst quantity needed for pinewood liquefaction was calculated as 3% of the organic content of pinewood for the initial liquefaction experiments and then it was optimised in order to have a high biomass to solvent ratio closer to 1:1. Then, this optimised value was used as a basis for other liquefaction experiments and it was optimised further. For rice husk, 0.2:1 biomass/solvent was used as it has low density, in order to ensure that there was enough solvent for good stirring of the reaction mixture. Unless mentioned otherwise, the catalyst quantity is always mentioned in terms of weight percentage of total biomass feed, throughout this thesis. The biomass to be used in liquefaction experiment was pre-treated by placing in a bag and spraying it with the solvent, enough to wet the biomass and then the biomass was placed in an oven at 80 °C for at least 30 minutes. This was done to soak the biomass with solvent and to reduce the thermal shock on the biomass when adding it to the reactor. Before some liquefaction experiments, the moisture from biomass was removed by heating it to 120 °C in an oven and keeping it at that temperature overnight.

This setup consists of a reactor with a bottom valve, mounted in a heating mantle supported by a tripod. The top end of the reactor was closed using a lid with 3 narrow and 1 wide inlet. One narrow inlet was used to insert a temperature sensor which was connected to a digital thermostat, into the reactor; the second narrow inlet was connected to a condenser through a dean stark. A metallic mesh was inserted into the neck of the dean stark to promote phase separation of the evaporated solvent and water mixture passing to the condenser. The third narrow inlet was used to feed the biomass into the reactor. The wide inlet was used to insert a stirrer into the reactor, which was driven by an electric motor. All the joints in this setup were hermetically sealed using high-temperature resistant grease. To start an experiment, a measured quantity of solvent was added to the reactor, the thermostat was set to 80 °C and the stirrer was switched on and set at a speed of around 180 rpm. When the temperature reached 80 °C, the pre-treated biomass was added to the reactor and the temperature in thermostat was set to 160 °C. When the reactor contents reach 160 °C, the measured quantity of catalyst was added to the reactor and the reaction timer was set to begin. After the planned reaction time, the heating and stirring are switched off and the contents of the reactor were allowed to cool down to ambient temperature. Then, one of the following two methods were used to separate the liquid from the solids. The first method was to simply separate the solids and liquid by filtration and then wash the solid residues using acetone to recuperate any bio-oil left; the filtrate was then distilled to remove the acetone and then added back to the bio-oil obtained. The second method was to add acetone to the entire reaction contents, mix them up and then filter, separate the solids, and distil the filtrate to remove acetone and obtain the bio-oil. Using the second method, it was possible to remove finer solids

from the bio-oils, which will be explained further in detail in Chapter 3.2. The solid residues obtained were heated to 80 °C to remove any acetone left and then cooled down in a desiccator before weighing. This weight was used to calculate the conversion of biomass in liquefaction experiments using the following formula.

$$\%\ Conversion = \left(\frac{Weight\ of\ biomass\ before\ liquefaction - Weight\ of\ residues\ obtained}{Weight\ of\ biomass\ before\ liquefaction}\right) * 100$$

2.2. Preliminary tests of combustion additives

In order to decrease the fine particles emission from biomass combustion, several additives are planned to be tested in a drop tube furnace at IST. For this purpose, the additives need to be screened initially. The additives selected for this initial screening phase were PentaErythritol Tetra Ester (hereafter referred to as 'TORR'), Kaolin, and TiO_2. TORR was selected due to its neopentane structure with ester chains on four end carbon atoms, which facilitates its use in multiple industrial applications such as lubricants, polymer cross-linking agents, etc. Hence, it was tested to determine if the four ester groups could trap smaller ash particles within its neopentane backbone. These additives were provided by a researcher from the research group 'CERENA' at IST. In order to test these additives, the biomass and additives were blended in a ball-mill for 15 minutes at 400 rpm. Two experiments were performed to test these blends. The first one was calcination in an oven. The second experiment was preliminary lab-scale combustion to simulate a combustion environment as shown in Figure 2. In these tests, biomasses and biomass-additive blends (with 3% and 6% additives with respect to total biomass) were combusted in the presence of a Particulate Matter (PM) meter with the capability of measuring concentration of particle size as low as 1 µm. The apparatus used for this purpose was DUSTTRAK-II-Aerosol-Monitor-8530 and it operates by laser scattering to provide concentration values of different fractions. In these preliminary tests, the assembly shown in Figure 2 was used, in which the suction line was placed in the path of the flue gas released in the combustion, as visible. It should be noted that in the treatment of results, the background values and the values influenced by the flame of the torch used to ignite the biomass were discounted.

Figure 2: Experimental setup for preliminary tests of biomass-additive blends

2.3. Characterisation techniques

The biomass feedstock used in liquefaction experiments, and preliminary combustion tests, the bio-oils and solid residues from liquefactions were characterised using Scanning Electron Microscopy, Energy Dispersive Spectroscopy, Calorimetry, Thermogravimetric analysis, Differential Thermogravimetric analysis, Calcination and Mid-Infrared Fourier Transform Infrared Spectroscopy. The samples were calcinated by heating from ambient temperature to 400 °C in 2 hours; then maintained at 400 °C for 3 hours; then heated up to 1000 °C in 3 hours; and finally maintained at 1000 °C for 3 hours. The calcinated samples were weighed after cooling down to ambient temperature from 1000 °C. The equipment used were: FTIR: PerkinElmer, Spectrum Two, mid-Infrared spectrometer equipped with a Pike Technologies MIRacle® Attenuated Total Reflectance (ATR) accessory; SEM-EDS: Analytical FEG-SEM-JEOL 7001F with Oxford light elements EDS detector (point and area analysis); Calorimetry: LECO AC500 analyser; Elemental analysis: The chemical composition data concerning carbon, hydrogen,and nitrogen were obtained via elemental analysis using an LECO TruSpec CHN analyser instrument while for sulphur, the determination was carried out in an LECO CNS2000; TGA: NESTZSCH model STA 449 F5, Jupiter Deckel Al2O3 Ø7mm Crucibles, 85µl and respective covers Deckel Pt / Rh 80/20 Ø7mm, 85µl Crucibles and Lids, Type III nitrogen with a purity of 99.999%; Calcination: Nabertherm P330 oven with temperature range of 30 to 3000 °C.

3. RESULTS AND DISCUSSION

3.1. Characterisation of biomass feedstock

The EDS images showed that pinewood is inhomogeneous, as shown in Figure 3. The elemental composition and GCV of the biomasses are tabulated in Table 2. It can be seen that the carbon, hydrogen content, and GCV of the aforementioned biomass feedstock are closer to each other except rice husk which has significantly low carbon content leading to a lower GCV. All these biomass have low sulphur and nitrogen content. Olive stone and olive bagasse have high moisture content whereas rice husk has the lowest moisture content. Pinewood has the lowest ash content; olive stone ranks one position above the lowest; olive bagasse and grape seeds have similar ash content; and rice husk has the highest as content which is almost 15 times that of pinewood. This high ash of rice husk is due to the high Si content which can be seen from EDS results of the calcinated rice husk in comparison to the EDS of calcinated pinewood, olive stone, and olive bagasse. This high Si content creates huge vitrification and agglomeration problems in direct combustion making it worthwhile to explore the feasibility of its liquefaction to produce a liquid fuel from rice husk with decreased ash content. On the other hand, olive stone and olive bagasse have high K content; and pinewood has high Ca content. Ca and K are known to be among the major precursors for formation of aerosols [Obernberger].

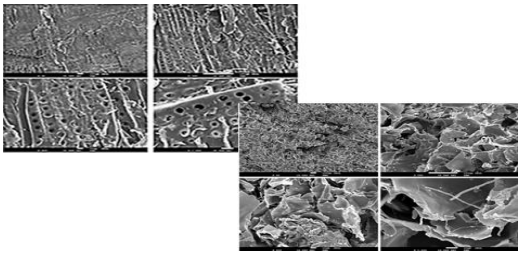

Figure 3: Inhomogeneity of pinewood on microscopic level: Different SEM images (left and right) of two random pinewood pieces, at same magnifications; Magnification in both left and right images are 50x, 250x, 500x, and 1000x from top left in counter-clockwise direction

Table 2: Elemental composition and gross calorific value of biomass feedstock

Biomass / Component	Pinewood	Olive stone	Olive bagasse	Grape seeds	Rice husk
Carbon*§	51.00	50.20	50.40	53	34.87£
Hydrogen*§	5.84	5.82	6.02	5.78	4.23£
Nitrogen*§	<1.26	<1.26	<1.26	1.7	<0.5£
Sulphur*§	<0.11	<0.11	<0.11	<0.11	<2£
Moisture§	10.50	18.10	20.60	11.3	7.80
Ash§	0.30	0.82	2.15	2.64	15.11
GCV (J/g)	20150	20370	21180	21170	14200#

* dry basis, § weight %, # [CFN], £ dry ash free basis

Figure 4 presents the TGA and DTG analyses of pinewood and olive stone between 0 and 600ºC, conforming to the norm. The TGA curves present the remaining weight as a function of the temperature whereas the DTG curves present the rate of fractional conversion. After the peak at temperatures below 100ºC due to the

moisture loss, the DTG curve for pinewood shows that its decomposition occurs between 150 ºC and 600ºC with two small peaks at 150ºC and 500ºC and with a large decomposition peak at 350ºC. Olive stone decomposes between 200 and 600ºC with and important peak at 300ºC slightly below the decomposition peak of pinewood. According to Jin et al. (2012), the peak temperature for cellulose decomposition occurs in the temperature range of 300 °C to 400 °C with a large decomposition peak at 340 °C; hemicellulose gets decomposed in the temperature range of 150 °C to 400 °C with a large decomposition peak at 200 °C; and the degradation of lignin occurred in the temperature range of 100 °C to 700 °C with a small degradation peak at 340 °C. It is worth noting that depending on the crystallinity of the samples, the decomposition peaks can vary significantly.

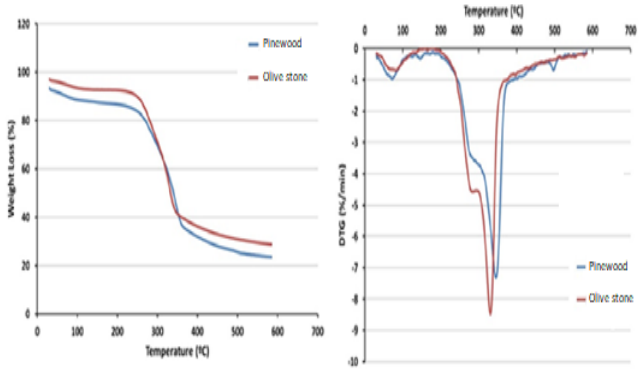

Figure 4: TGA (left) and DTG (left) analyses of pinewood and olive stone

Figure 5 presents the FTIR spectra of the biomass feedstock which can be analysed to interpret the functional groups present indicated by the characteristic absorption peaks in the literature. [(Zou et al., 2009 cited by Braz, A., 2015), (Sills & Gossett, 2011), (Adapa et al., 2011)]. As seen in Figure 36, all the spectra exhibit peaks at the similar wavelengths but with different heights. Actually, the spectra have the typical bands of cellulosic biomasses such as at 3200 - 3500 cm^{-1} due to the stretching vibration of hydroxyl groups [Zou, et al., 2009], at 2800-3000 cm^{-1} which corresponds to the C-H stretching [(Grilc et al., 2015), (Bui et al., 2015)], the peaks at 1510-1600 cm^{-1} that may be related to the lignin's aromatic rings stretching [(Chen & Lu, 2009), (Zou, et al., 2009)] and at 1000-1200 cm^{-1} due to C-O stretching of the cellulose [(Zhang et al., 2012), (Bui et al., 2015)].

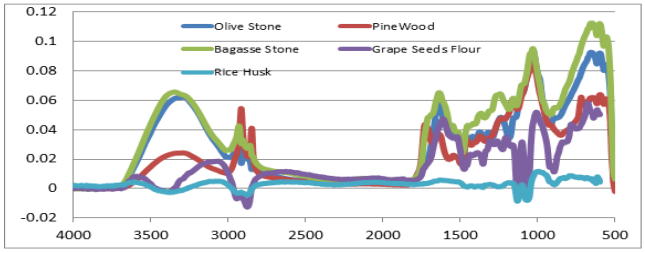

Figure 5: FTIR spectra of biomass feedstock

3.2. Liquefaction experiments

When the liquefied products were washed with acetone to extract the organic fraction and to improve the separation of the solids, it leads to the increase of amount of residue obtained, thus lowering the conversion. Having in mind the economic viability of scaling up the biomass liquefaction to an industrial scale, it is crucial to use high values of the biomass to solvent ratio. However, it is also necessary to have a certain minimum amount of liquid in the reactor to ensure the continuation of reaction, proper stirring of the reaction mixture, and prevention of bio-oils from becoming too viscous. Therefore, in some of the experiments the addition of the biomass was carried out in several stages to increase the biomass to solvent ratio as much as possible. However, carrying out liquefaction in incremental stages takes more time to produce similar conversions as that of single stage reactions and if carried out with less reaction time, the conversion is much lower than that of single stage reactions. The viscosities of products from different stages of two such experiments of OS and PW are shown in Figure 6. It can be seen from this figure that the viscosity of liquefied products increased with the increase in number of stages, which was slow till third stage for pinewood and fifth stage for olive stone. After these stages, the increase in viscosity is rapid. This augment of viscosity may be due to the occurrence of re-polymerisation reactions and/or due to more solids getting suspended in the liquid. However, viscosity of the final liquefaction products from these experiments after washing with acetone to remove, as completely as possible, the solids from bio-oils, was around 0.3 P between 25 to 50 °C and decreased below 0.1 P above 50 °C. The viscosity of these bio-oils is comparable to that of Heavy gas oil from North Sea light crude (0.07 P at 99 °C) and that of Heavy gas oil from the Alaskan North slope crude (0.13 P at 37 °C) [ABS, 1984] These heavy gas oils are used as liquid fuel in many thermal power plants in the USA, Canada, and many European countries [ABS, 1984]. It can be inferred from these data that the viscosities of these bio-oils are in the suitable range for industrial applications.

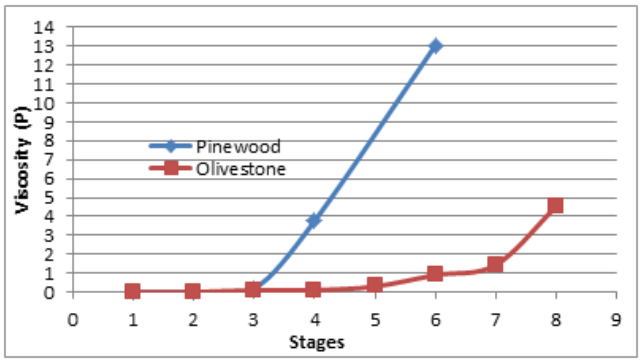

Figure 6: Viscosity of liquefied products from pinewood and olive stone at different stages of reaction; Conditions: PW – 0.72:1 B/S, 24.25 hours reaction time, 5.58% catalyst (total biomass basis), OS – 1.19:1 B/S, 22 hours reaction time, 4.5% catalyst (total biomass basis)

The observed increase of viscosity during the liquefaction reaction and/or during storage of the bio-oils may be due to the occurrence of re-polymerisation reactions. Therefore, the effect of the addition of hydroquinone (HQ) was studied based on a hypothesis that this compound can hinder these reactions by acting as a radical scavenger, thus stabilizing the polymerization initiators. Figure 7 shows the relationship between pinewood liquefaction conversion and the quantity of the stabilizer hydroquinone added.

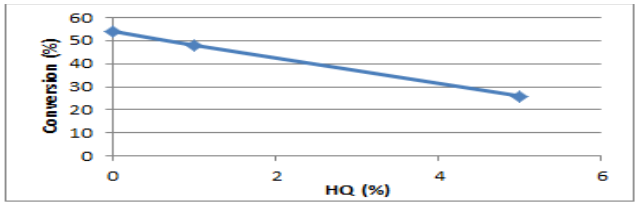

Figure 7: Effect of HQ quantity on conversion of pinewood liquefaction; Conditions: 1:1 B/S, 5.6% catalyst (total biomass basis), 3 hours reaction time

It can be inferred from Figure 7 that the conversion decreases almost linearly with the increase in HQ used in the reaction irrespective of the reaction time. Also, the conversion dropped with increase in use of HQ for olive stone liquefaction. It can be concluded that using HQ as a stabilizer for liquefaction considerably

decreases the conversion. For pinewood liquefaction, the use of catalyst in any quantity less than 5% of the organic content of pinewood (which is 5.6% of the total biomass) always led to a conversion less than 10%, irrespective of other reaction parameters such as reaction time and biomass/solvent ratio. However, since no reactions were carried out using a catalyst concentration higher than 5.6% the optimum catalyst amount could be equal to or more than 5.6% of the biomass fed. Also, it must be emphasized that increase in catalyst quantity leads to increase in cost of liquefaction. Concerning olive stone liquefaction, catalyst quantities below 2.4% of the organic content of olive stone (3% of the total biomass) led to incredibly low conversions independent of other reaction parameters. The conversion increased steeply from 3% catalyst to 4.5% catalyst, after which it plateaued. This is illustrated in Figure 8.

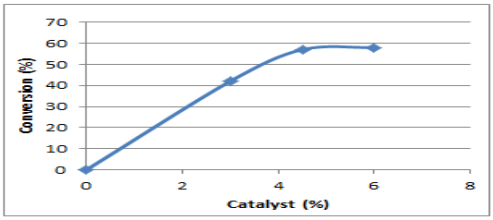

Figure 8: Conversion of olive stone liquefaction at different catalyst quantities; Conditions: 1:1 B/S, 4 hours reaction time.

Also, when olive stone liquefaction was scaled up from 50g:50g of biomass/solvent to 1500g:1500g biomass/solvent, with 4.5% catalyst, it resulted in 49% conversion, around 8% less than that of its smaller scale counterpart, which is not much of a loss for a scaled up reaction. Hence, the optimum amount of catalyst for olive stone liquefaction is 4.5% of the biomass fed. The same 4.5% catalyst was used for liquefaction experiments of grape seeds and rice husk. The reaction time is an important variable and previous results have shown that increasing the time does not necessary lead to a higher conversion [Braz, A., 2015]. In fact, for example, an increase in the reaction time can favour the re-polymerisation reaction. Hence, this variable was studied. For pinewood, the optimum reaction time was found to be between 3 and 5 hours whereas it was 4 hours for olive stone. The conversion vs. reaction time for olive bagasse shown in Figure 9 indicates that the conversion increases with time and above 2 hours, the conversion values are in the same range. The conversion is almost half of that obtained for pinewood and olive stone liquefactions. Hence, olive bagasse liquefaction has to be optimized further by changing biomass/solvent ratio and catalyst quantity.

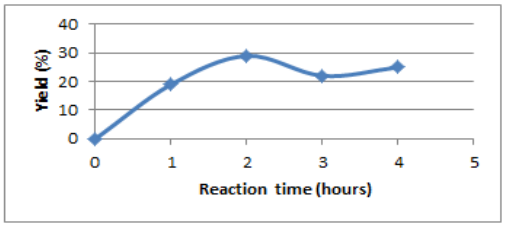

Figure 9: Conversion vs. Reaction time for olive bagasse liquefaction Conditions: 1:1 B/S, 4.5% catalyst (total biomass basis)

The quantity of catalyst and reaction time of liquefaction reactions were optimised while trying to maintain a high biomass to solvent ratio. No firm conclusions can be derived from the obtained results, as to the effect of biomass to solvent ratio on conversion of pinewood and olive stone liquefaction. However, it can be inferred from rice husk liquefaction results that lower biomass to solvent ratio (5 times lower) had to be used to obtain conversions similar to that of pinewood and olive stone liquefaction. Also, using the same biomass to solvent ratio (1:1) for olive bagasse gives significantly lower conversions while it is almost negligible for grape seeds. This could be due to the higher inorganic content of olive bagasse and grape seeds compared to that of pinewood and olive stone. From these results, it can be hypothesised that it is necessary to decrease biomass to solvent ratio for biomass with high inorganic content, in order to achieve higher conversions. Liquefaction of olive bagasse exhibited much lower conversion than pinewood and olive stone liquefaction as discussed earlier. Liquefaction of grape seeds with 4.5% catalyst and 1:1 biomass/solvent ratio led to a low conversion of 8% irrespective of increasing the reaction time till 6 hours. Also, concerning rice husk, the conversion was 58%, with 0.2:1 biomass/solvent ratio, 5 hours reaction time and 4.5% catalyst. When the liquefied product from this reaction was used as solvent in another reaction with same reaction parameters, the conversion dropped to 23%. So, the overall conversion for an overall biomass/solvent ratio of 0.4:1 and overall reaction time of 10 hours was 40%. Notwithstanding the fact that the elemental compositions of olive bagasse and grape seeds are not so different from olive stone and pinewood, it must also be taken into account that olive bagasse and grape seeds have inorganic content more than twice that of pinewood and olive stone whereas rice husk has about 15 times more inorganic content than pinewood and olive stone. Considering these aspects, the liquefactions of these biomasses need to be investigated and optimized further by changing biomass/solvent ratio, catalyst quantity, and reaction time. In order to estimate the calorific value of bio-oils from different biomass, representative samples were made by mixing products from different experiments in proportions due to inadequate quantity of any one sample. The results are shown in Figure 10

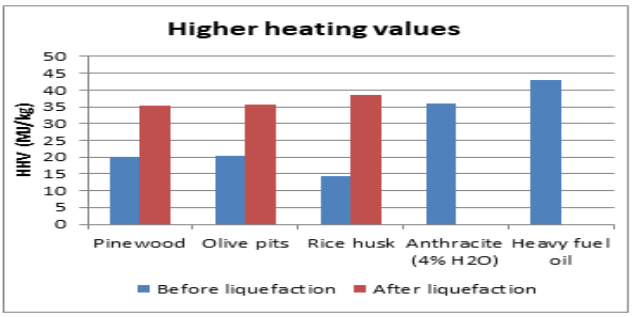

Figure 10: HHV of bio-oils in comparison to biomass and common fuels

The GCV of bio-oils are significantly higher than that of their biomass feedstock. Also, the GCV of bio-oils from PW, OS and RH are higher than that of Ethanol and comparable to that of anthracite with 4% water while these are lower than the GCV of biodiesel and heavy fuel oil. It may be hypothesized that the high GCV of C1 and C2 may be suspected to be due to high amounts of unreacted solvent since their GCV are closer to GCV of 2EH [BASF]. But, the lower GCV of C3 which had insignificantly low conversion and consequently high amounts of unreacted 2EH disproves this hypothesis. FTIR spectroscopy was performed for the bio-oils from different biomass feedstock. These FTIR spectra are shown in Figure 11. Though FTIR analysis of liquefied products is not as pertinent as measurements such as viscosity, calorific value, inorganic content, and proximate analysis, to using liquefied products in direct industrial combustion, the following qualitative inferences from the above FTIR spectra could be useful in further research in optimizing the liquefaction reactions to produce specific chemical products.

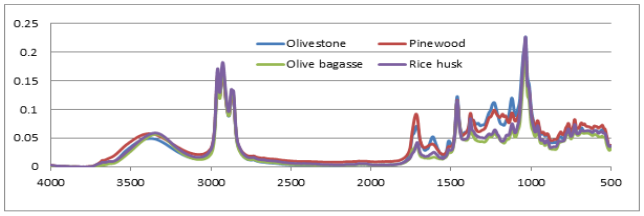

Figure 11: FTIR spectra of liquefied products from OS, PW, OB, and RH; Conditions: OS – 1:1 B/S, 4 hours reaction time, 4.5% catalyst (total biomass basis), OB - 1:1 B/S, 3 hours reaction time, 4.5% catalyst (total biomass basis), PW - 1:1 B/S, 5 hours reaction time, 5.6% catalyst (total biomass basis), RH - 0.2:1 B/S, 5 hours reaction time, 4.5% catalyst (total biomass basis)

The peak at 3422 cm^{-1} is the characteristic O-H stretch indicating the presence of alcohol groups. However, it must be taken into account that this also includes the alcohol groups from the unreacted solvent since it was not removed before the measurement of these spectra. The peak in the characteristic C-H stretching region from 2800 to 3000 cm^{-1} indicates the presence of aromatic groups. The spectral region with the C=O stretching peak at 1730 cm^{-1} indicates the presence of aldehyde and ketone groups. The peak at 1466 cm^{-1} indicates the presence of compounds formed by C-H deformation of lignin. The absence of any prominent peak in the region 875 to 930 cm^{-1} which is the characteristic of glycosidic linkages of cellulose, hemicellulose, and lignin indicates that the breakage of glycosidic bonds between the monomeric units of the biomasses is complete. Further analysis using FTIR or other methods such as GC-MS is needed to firmly substantiate any more claims as to the qualitative and quantitative analysis of the liquefied products. The analysis of the inorganic content of the liquefaction residues showed that 60 to 70% of the inorganic content of the biomasses was removed using liquefaction as shown in Figure 12.

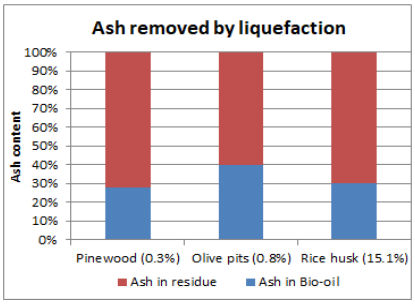

Figure 12: Inorganic content removed by liquefaction

The remaining inorganic content in the liquefied products may be due to two reasons: the inorganic particles are less than 5 to 13 µm in size and/or they are trapped between bigger polymeric compounds in the liquefied product. If this smaller particle size is the sole reason, then it should be possible to produce a liquefied product that is completely free of inorganic content by methods such as ultra-filtration although it finally boils down to economic feasibility of such filtration processes. As for the inorganic particles that could be trapped between the polymeric components, ultrasonic agitation combined with solvent extraction could be a plausible solution.

3.3. Preliminary tests results for combustion of biomass-additive blends:

The calcination tests results were inconclusive indicating that this way of testing the additives is not the right approach. The preliminary combustion tests performed for TORR may not be accurate since the flame got extinguished often possibly due to drafts. Also, the results from pinewood need to be treated with caution as the flue gas produced contained a lot of soot with low density unburnt pinewood particles getting elutriated. The olive stone results showed that TiO_2 decreased PM_1 and increased $PM_{2.5}$ and PM_4, indicating the possibility of aggregation. Thus, TiO_2 could be a promising additive. Figure shows the PM emissions from these tests.

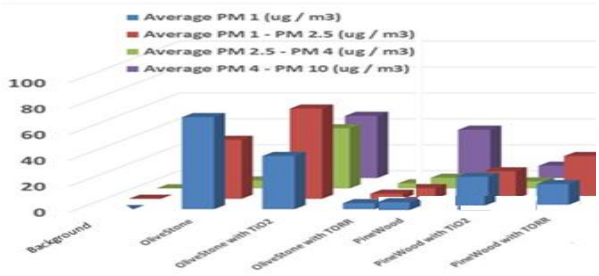

Figure 13: PM emissions from the preliminary combustion tests

3.4. Aspen simulation results

The values of typical input parameters are: Flue gas inlet flow rate – 4000 m^3/h, temperature – 200 °C, pressure – 1 atm, and maximum allowed pressure drop – 150 mm-water. The flue gas composition is unknown and hence a reasonable composition was assumed based on data from literature [(Xu et al., 2003), (Liu et al., 2010)]: H_2O – 6.20%, NO_2 – 0.03%, O_2 – 4.40%, N_2 – 76.81%, NO – 0.01%, SO_2 – 0.04%, CO – 0.01%, and CO_2 – 12.50%. The ash loading in the flue gas was assumed to be 150 mg/Nm^3 based on data from literature for woody biomass combustion [Hasler et al., 1998]. However, to evaluate the influence of this parameter on efficiency, a value of 1500 mg//Nm^3 was also used to simulate multicyclones. Simulations were performed for three types of Torbel's cyclones – Helical cyclone, spiral cyclone, and multicyclones. The length of vortex finder for Torbel's helical and spiral cyclones were not given. Hence, values which were optimised using Aspen to give maximum efficiencies were used to run simulations. Also, the inlet angle for spiral cyclone was not given. Hence, it was assumed to be 0° since it gave the maximum efficiency.The real PSD of the flue gas is also unknown. Hence, the PSD suggested by Torbel, based on a literature survey, was used to perform the simulations. This PSD is delineated in Table 4. Mothes-Loffler (ML) model was used since it gives more realistic results due to more accurate turbulence and particle diffusion calculations [Aspen]. Shepherd & Lapple model (SL) was also used to determine the effect of changing the inlet length inside the cyclones. Both SL and ML gave similar results for the separation efficiencies, with up to 0.01% difference for 150 mg/Nm^3 ash loading and up to 5% difference for 1500 mg/Nm^3 ash loading. The vane constant is a measure of the length to which the gas inlet of the cyclone extends inside the cyclone [Aspen]. When the vane constant is 16, the inlet does not extend beyond the wall of the cyclone whereas when it is 7.5, the inlet extends inside the cyclone till the axis [Aspen]. Decreasing the vane constant from 16 to 7.5 causes a 53% decrease in pressure drop, independent of the number of cyclones used and of the ash loading. Hence, using an inlet vane, to extend the gas inlet till the axis of the cyclone, can reduce the pressure drop by half in Torbel's multicyclones system. However, changing the vane constant has no effect on separation efficiency and PM emissions. As expected, due to the reduction of the velocity, the pressure drop significantly decreases with increase in the number of cyclones. However, even for a multicyclone system with T number of cyclones, as prescribed by Torbel (value of T is mentioned in Annex in Table 24), with Torbel dimensions, the pressure drop is far below 150 mm-water, which is Torbel's limit. Concerning multicyclones, simulations were performed using the number of cyclones prescribed by Torbel (T) and also different numbers of cyclones. Systems with less than T/3 cyclones led to an inlet velocity more than 30 m/s, which is the highest allowable limit in Aspen.

Table 4: PSD of flue gas used to perform simulations

Lower limit (µm)	Upper limit (µm)	Mass fraction	Cumulative mass
0.05	0.15	0.01	0.01
0.15	0.25	0.03	0.04
0.25	0.75	0.04	0.08
0.75	2.25	0.04	0.12
2.25	7.75	0.15	0.27
7.75	12.25	0.40	0.67
12.25	37.75	0.20	0.87
37.75	82.25	0.10	0.97
82.25	277.75	0.03	1.00
SMD (µm) 2.29			
D_{50} (µm)10.34			

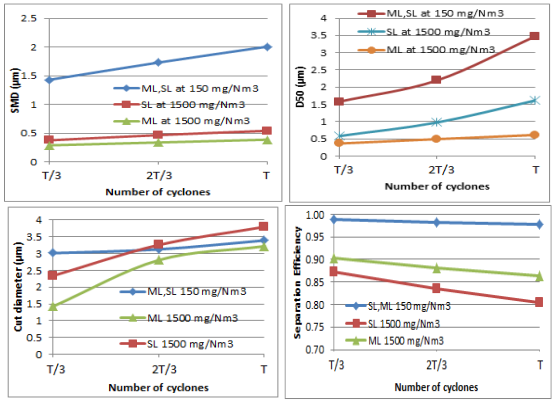

Figure 14: SMD, D_{50}, D_{cut}, and η results for multicyclones; ML: Mothes - Loffler model, SL: Shepherd & Lapple model

From the above Figure 14, it can be seen that all the performance parameters improve with decrease in number of cyclones from T to T/3, with increase in pressure drop and inlet velocity. The results for simulation of helical, spiral, and Stairmand HE suggested by Aspen are shown below in Figure 15. The helical cyclones analysed here perform better than spiral cyclones in all the above scenarios with higher overall separation efficiencies and higher fractional efficiencies. However, the efficiency of spiral cyclones can be improved further by decreasing the inlet height and width thus increasing the inlet velocity till 28 m/s, which is Torbel's limit for spiral cyclones. The cut diameters and SMD of the spiral cyclone are higher than those of helical cyclones but this reverses when the inlet height and width of spiral cyclone are decreased such that the inlet velocity is closer to 28 m/s. For the given process conditions, Aspen gives an optimised design of Stairmand High Efficiency cyclone, which has better overall separation efficiency, fractional efficiencies, smaller cut diameter and SMD. Also, the pressure drop for this proposed design is below 150 mm-water, the limit.

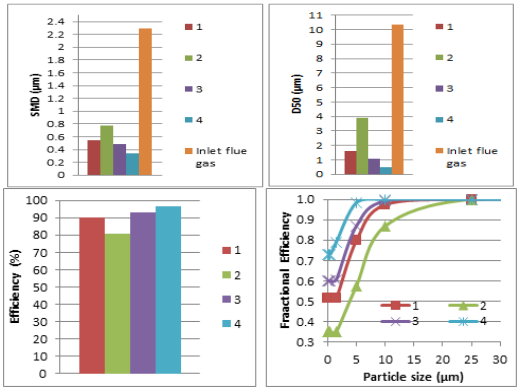

Figure 15: SMD, D_{50}, η, and η_i for 1, 2, 3, and 4 - respectively Torbel's helical, spiral, spiral with reduced inlet dimensions, and Aspen-proposed Stairmand High Efficiency cyclones.

4. CONCLUSIONS

To summarise, in this work, liquefaction of the biomasses – pinewood, olive stone, olive bagasse, grape seed, and rice husk was investigated as a pre-treatment before combustion in order to: i) decrease fine particles emission from biomass combustion and ii) produce a liquid biofuel that can be easily burned. The liquefaction conditions for pinewood and olive stone were optimized to use high biomass to solvent ratio of 1:1 (w/w). The solvent used was 2-Ethylhexanol and at this ratio pinewood and olive stone yielded around 55% conversion of the initial biomass. To achieve this conversion, the required reaction time at 160ºC is between 3 to 5 hours for pinewood whereas it is 4 hours for olive stone. The catalyst used was p-Toluene sulfonic acid and the concentration needed for this conversion is 5.6% for pinewood and 4.5% for olive stone. The liquefaction of olive stone was successfully scaled up to use 15 times more biomass feed than the optimised experiments proving its potential to be scaled up further. Olive bagasse gave low conversions of around 20% with the same conditions as olive stone whereas grape seeds gave insignificant conversions. Therefore, olive bagasse and grape seeds need to be investigated further to establish optimum liquefaction conditions. Rice husk gave similar conversions of around 55% as pinewood or olive stone but with a less biomass to solvent ratio (0.2:1) because of its low density. This behaviour of rice husk may be due to its high inorganic content which is 15 times higher than that of pinewood and olive stone. Thus, rice husk liquefaction is promising and has to be studied further using different conditions. Concerning the calcination of the liquefaction residues the results showed that 60 to 70% of the inorganic content of the biomass was removed by liquefaction. It is important to note that the solids left in the bio-oils may be due to the presence of solids in suspension due to an inefficient solid-liquid separation and/or due to the particles caught up between large molecules in the bio-oils. The higher heating values of the bio-oils from pinewood and olive stone liquefaction were 35.3 and 35.6 MJ/kg which is closer to that of anthracite with 4% H_2O (36 MJ/kg) and biodiesel (39-41 MJ/kg) and less than the higher heating value of heavy fuel oil (43 MJ/kg). Their viscosities (~0.3 P at 25 °C and <0.1 P above 50°C) were closer to that of heavy gas oil fractions obtained from Alaskan North Slope (0.13 P at 37 °C) and North Sea Light crudes (0.07 P at 99 °C). These results indicate the suitability of these bio-oils to be used in industrial combustion applications. Preliminary tests were performed to evaluate the efficacy of the additives, PentaErythritol Tetra Ester, Kaolin and Titanium dioxide, to reduce fine particle emissions from biomass combustion. The first attempt was to evaluate their effect in the amount of inorganic residue obtained after calcination. However, the tests performed for this purpose turned out to be inconclusive, proving this method is not effective. TGA analyses will be also carried out as soon as possible. The preliminary lab-scale combustion tests performed with these additives proved that TiO_2 can be a promising additive to decrease particulate emissions in flue gases, especially PM_1 emissions. The decrease of PM1 emissions was accompanied by an increase of $PM_{2.5}$ and PM_4 which may be an indication of the formation of aggregates. On the other hand, these combustion tests turned out to be a useful basis that was given to Torbel to set up a laboratory scale installation to test the performance of these additives in more controlled environment. Finally, Aspen Plus V8.4 was used to rate the performance of Torbel's multicyclone system, spiral cyclone and helical cyclone designs at given process conditions and under reasonable assumptions for unknown parameters. It was found that Torbel's multicyclones performed better for removing PM emissions in flue gases than helical cyclone, which in turn performed better than Torbel's spiral cyclone. Decreasing the number of cyclones in the multicyclones system from Torbel, specified value identified as T, to T/3 resulted in an increase in the efficiency. Even though this increase was small

(1.1%) at an ash loading of 150 mg/Nm^3, it increased further to 7% when the ash loading was increased by one order of magnitude. This indicates that decreasing the number of cyclones from T to T/3 has significant advantage at high ash loading of flue gas. Also, adding an inlet vane to cyclones extending from the point of intersection of gas inlet and cyclone wall till the axis of cyclone (vane constant is 7.5) reduced the pressure drop by a half. Concerning Torbel's spiral cyclone, it was possible to improve its performance by decreasing the inlet height by 12.5% and inlet width by 35%. This change resulted in 12% increase in overall separation efficiency and 64% decrease in PM emissions when compared to the spiral cyclone with Torbel's dimensions. A set of iterations were performed in design mode with the same input parameters in order to determine the optimum cyclone dimensions suggested by Aspen. Aspen suggested the use of a Stairmand High Efficiency cyclone instead of Torbel's spiral and helical cyclones. This cyclone showed 7% higher efficiency than Torbel's helical cyclone and 16% more efficiency than Torbel's spiral cyclone. In all these cases, the pressure drop was less than Torbel's limit, 320 mm water. Also, at an ash loading of 150 mg/Nm^3, the PM emissions from all these cyclones were less than 50 mg/Nm^3, which is Torbel's target. However, at an ash loading of 1500 mg/Nm^3, the minimum possible PM emissions achievable was 142 mg/Nm^3.Since the output gas stream downstream of this cyclone has a high volumetric flow rate and more aerosols, cyclones cannot be used to decrease the PM emissions further from 142 to 50 mg/Nm^3 and hence other equipment such as small bags filter or ESP is needed for this purpose. To conclude, for the given process conditions and for the studied particles loadings, the order of preference of the cyclone separators is as follows: Torbel's multicyclones system with T/3 cyclones and vane constant 7.5 > Torbel's multicyclone system with T cyclones > Stairmand HE proposed by Aspen > Torbel's Helical cyclone > Torbel's spiral cyclone with reduced inlet height and width > Torbel's spiral cyclone.

5. ACKNOWLEDGEMENTS

The author would like to thank his thesis supervisors, Prof. Joana and Dr. José for their guidance and help, without which completing this thesis would have been a Herculean task. The author is thankful to Dr. Margarida Mateus for her valuable inputs and her help with analyses. Also, his gratitude goes to Dr. Nuno Canha from IST Center of Sciences and Nuclear technologies for providing equipment and help for measuring PSD of emissions during combustion experiments. He would also like to thank Prof. Bordado for his amazing ideas regarding additives. Finally, the author would like to express his gratitude for the company Torbel, for providing the needed raw materials and the necessary data for this work which was performed within a project 'Partiless', a collaboration of IST and Torbel.

6. BIBLIOGRAPHY

ABS – American Bureau of Shipping, 'Notes on Heavy Fuel Oil', 1984; 16/10/2017.

Adapa, P. K.; Schonenau, L. G.; Canam, Thomas; and Dumonceaux, T., 2011, 'Quantitative Analysis of Lignocellulosic Components of Non-Treated and Steam Exploded Barley, Canola, Oat and Wheat Straw Using Fourier Transform Infrared Spectroscopy', Faculty Research & Creative Activity. 107.

Aspen – Aspen Plus V8.4 help manual; 16/10/2017

Bäfver, L.; Boman, C.; and Rönnbäck, M., 2011, 'Reduction of particle emissions by using additives', Central European Biomass Conference, Graz, Austria.

Bajpai, P., 2016, 'Pretreatment of Lignocellulosic Biomass for Biofuel Production', Chapter 2: 7.

BASF – Technical specifications of 2-Ethylhexanol by BASF;

Boman, C.; Dan Boström, D.; Jonathan Fagerström, J.; Marcus Öhman, M.; Ida-Linn Näzelius, I.L.; and Linda Bäfver, L., Report on 'Fuel additives and blending as primary measures for reduction of fine ash particle emissions – state of the art', 2012, ERA-NET FutureBioTec.

Braz, A., 2015, 'Liquefacção de Madeira de Pinho', Dissertation for Master's in Chemical Engineering, Instituto Superiro Técnico.

Bui, N.Q.; Fongarland, P.; Rataboul, F.; Dartiguelongue, C.; Charon, N.; Vallée, C.; and Essayem, N., 2015, 'FTIR as a simple tool to quantify unconverted lignin from chars in biomass liquefaction process: Application to SC ethanol liquefaction of pine wood', Fuel Processing Technology 134: 378-386.

Chen, F.; and Lu, Z., 2009, 'Liquefaction of wheat straw and preparation of rigid polyurethane foam from the liquefaction products', Journal of Applied Polymer Science 111(1): 508–516

Chew, J.J.; and Doshi, V., 2011, 'Recent advances in biomass pretreatment – Torrefaction fundamentals and technology', Renewable and Sustainable Energy Reviews 15(8): 4212-4222.

Clarke, S. and Preto F., 'Biomass Densification for Energy Production', Factsheet, June 2011.

Clift, R.; Ghadiri, M.; and Hoffman, A.C., 1991, 'A critique of two models for cyclone performance', AIChE Journal 37(2): 285-289.

Cuevas, M.; Sánchez, S.; Bravo, V.; Cruz, N.; and García, J.F., 2009, 'Fermentation of enzymatic hydrolysates from olive stones by Pachysolen tannophilus', J. Chem. Technol. Biotechnol. 84: 461–467

Davidsson, K.O.; Steenari, B.M.; and Eskilsson, D., 2007, 'Kaolin Addition during Biomass Combustion in a 35 MW Circulating Fluidized-Bed Boiler', *Energy Fuels 21*(4): 1959–1966

Dirgo, J.; and Leith, D., 1985, 'Cyclone Collection Efficiency: Comparison of Experimental Results with Theoretical Predictions', Aerosol Science and Technology 4(4): 401-415.

Elsayed, K., 2011, 'Analysis and Optimization of Cyclone Separators Geometry using RANS and LES methodologies', Doctoral thesis, Department of Mechanical Engineering, Vrije Universiteit Brussel.

FAO - 'Unified Bioenergy Terminology', Food and Agricultural Organization Forestry Department's Wood Energy Programme, December 2004; ftp://ftp.fao.org/docrep/fao/007/j4504e/j4504e00.pdf; 16/10/2017

FAO – Food and Agricultural Organization of the United Nations, 'The research progress of biomass pyrolysis processes'; http://www.fao.org/docrep/t4470E/t4470e0a.htm; 16/10/2017

Fournel, S.; Palacios, J.H.; Godbout, S.; and Heitz, M., 2015, 'Effect of Additives and Fuel Blending on Emissions and Ash-Related Problems from Small-Scale Combustion of Reed Canary Grass', Agriculture 5: 561-576

Grilc, M.; Likozar, B.; and Levec, J., 2015, 'Kinetic model of homogeneous lignocellulosic biomass solvolysis in glycerol and imidazolium-based ionic liquids with subsequent heterogeneous hydrodeoxygenation over NiMo/Al_2O_3 catalyst', Catalysis Today 256(2): 302-314

Höfer, I.; and Kaltschmitt, M., 2017, 'Effect of additives on particulate matter formation of solid biofuel blends from wood and straw', Biomass Conversion and Biorefinery 7(1): 101-116.

Hu, S.; Luo, X.; and Li, Y., 2014, 'Polyols and Polyurethanes from the Liquefaction of Lignocellulosic Biomass', ChemSusChem 7(1): 66–72.

Hu, S.; Wan, C.; and Li, Y., 2012, 'Production and characterization of biopolyols and polyurethane foams from crude glycerol based liquefaction of soybean straw', Bioresource Technology 103(1): 227-233.

Kobayashi, M.; Asano, T.; Kajiyama, M.; Tomita, B., 2004, 'Analysis on residue formation during wood liquefaction with polyhydric alcohol', Journal of Wood Science 50(5): 407-414.

Li, Y.; Luo, X.; and Hu, S., 2015,'Bio-based Polyols and Polyurethanes', SpringerBriefs in Green Chemistry for Sustainability, ebook, chapter 3.3: 52.

Mateus, M.M.; Carvalho, R.; Bordado, J.C.; and Santos, R.J.D, 2015, 'Biomass acid-catalyzed liquefaction – Catalysts performance and polyhydric alcohol influence', Data in Brief 5: 736-738, Elsevier open access article.

Mateus, M.M.; Guerreiro, D.; Ferreira, O.; Bordado, J.C.; and Santos, R.G.D., 2017, 'Heuristic analysis of Eucalyptus globulus bark depolymerization via acid-liquefaction', Cellulose 24:659–668.

Mateus, M.M.; Ventura, P.; Rego, A.; Mota, C.; Castanheira, I.; Bordado, J.M.; and Santos, R.J.D., 2017, 'Acid Liquefaction of Potato (Solanum tuberosum) and Sweet Potato (Ipomoea batatas) Cultivars Peels – Pre-Screening of Antioxidant Activity/Total Phenolic and Sugar Contents', BioResources 12(1): 1463-1478.

Ninomiya, Y.; Wang, Q.; Xu, S.; Mizuno, K.; and Awaya, I., 2009, 'Effect of Additives on the Reduction of $PM_{2.5}$ Emissions during Pulverized Coal Combustion', *Energy Fuels 23*(7): 3412–3417.

NPTEL – Chemical Engineering – Chemical Engineering Design II – Module #5, an open course by Indian Institute of Technology and Indian Institute of Science, pp-3,4.

Nussbaumer, Th.; and Hasler, Ph., 1998, 'Particle Size Distribution of the Fly Ash from Biomass Combustion', Biomass for Energy and Industry, 10th European Conference and Technology Exhibition, Würzburg, Germany.

Obernberger, I., 'Fly ash and aerosol formation in biomass combustion processes – an introduction', Presentation, Institute for Resource Efficient and Sustainable Systems, Graz University of Technology.

Rachel-Tang, D.Y.; Islam, A.; and Taufiq-Yap, Y.H., 2017, 'Bio-oil production via catalytic solvolysis of biomass', RSC Adv. 7: 7820.

Tarelho, L.; Monteiro, C.; Lopes, M.; Monteiro, A.; Machado, L.; Amaral, J.; and Borrego, C., 2011, 'Forest biomass resources for industrial energy conversion in Portugal', 19th European Biomass Conference and Exhibition, Berlin, Germany.

UF - 'Aerosol Science and Engineering – Learning about cyclones', a course by University of Florida; http://aerosol.ees.ufl.edu/cyclone/section01.html; 16/10/2017

Wang, L.; Hustad, J.E.; Skreiberg, Ø.; Skjevrak, G.; and Grønli, M., 2012, 'A Critical Review on Additives to Reduce Ash Related Operation Problems in Biomass Combustion Applications', Energy Procedia 20: 20-29

Wiinikka, H.; Grönberg, C.; Öhrman, O.; and Boström, D., 2009, 'Influence of TiO_2 Additive on Vaporization of Potassium during Straw Combustion', *Energy Fuels* 23(11): 5367–5374

Xi, D.; Zhou, R.; Zhou, R.; Zhang, X.; Ye, L.; Li, J.; Jiang, C.; Chen, Q.; Sun, G; Liu, Q.; and Yang, S., 2017, 'Mechanism and optimization for plasma electrolytic liquefaction of sawdust', Bioresource Technology 241: 545-551.

Xu, X.; Song, C.; Wincek, R.; Andresen, J.M.; Miller, B.G.; and Scaroni, A.W., 2003, 'Separation of CO2 from Power Plant Flue Gas Using a Novel CO2 "Molecular Basket" Adsorbent', Fuel Chemistry Division Preprints 48(1): 162.

Yamada, T.; and Ono, H., 1999, 'Rapid liquefaction of lignocellulosic waste by using ethylene carbonate', Bioresource Technology 70: 61–67.

Zhang, T.; Zhou, Y.; Liu, D.; and Petrus, L., 2007, 'Qualitative analysis of products formed during the acid catalyzed liquefaction of bagasse in ethylene glycol', Bioresource Technology 98: 1454-1459.

Zhang, W.; Liu, H.; Hai, I.U.; Neubauer, Y.; Schröder, P.; Oldenburg, H.; Seilkopf, A.; and Kölling, A., 2012, 'Gas cleaning strategies for biomass gasification product gas', International Journal of Low-Carbon Technologies 7: 69–74.

Zou, X.; Qin, T.; Huang L.; Zhang, X.; Yang, X.; and Wang, Y., 2009, 'Mechanisms and Main Regularities of Biomass Liquefaction with Alcoholic Solvents', Energy Fuels 23: 5213-5218.